

## **Title: Material deprivation is associated with neural resilience for late-life depression**

Wei Zhang\*, Janine D. Bijsterbosch\*

Department of Radiology, Washington University School of Medicine, St. Louis,  
Washington University School of Medicine, St. Louis

\* Corresponding authors: WZ; JDB

**Email:** [weiz@wustl.edu](mailto:weiz@wustl.edu); [janine.bijsterbosch@wustl.edu](mailto:janine.bijsterbosch@wustl.edu)

**Author Contributions:** WZ and JDB designed the study; WZ analyzed the data; WZ drafted the paper and DB provided critical feedback.

**Competing Interest Statement:** No competing interests.

**Keywords:** late-life depression, material deprivation, neural resilience, neuroanatomical signatures

1 **Abstract**

2 Late-life depression (LLD) is a major source of global morbidity and mortality,  
3 influenced by multiple risk factors. Yet, a major challenge is to quantify the  
4 degree of resilience or vulnerability to LLD at the individual level, which could  
5 offer neurobiological insight and ultimately inform future interventions and  
6 treatment. Here, applying a non-parametric regression model to the UK Biobank  
7 data (N=1,988), we quantified brain-based resilience and vulnerability to LLD and  
8 tested whether risk factors could explain individual differences in the estimated  
9 magnitude of such neural resilience and vulnerability. Our results show that  
10 social isolation was positively associated with the median magnitude of neural  
11 vulnerability whereas material deprivation was negatively associated with the  
12 greatest neural resilience (top 10 percentile). These results together highlight the  
13 importance of social interaction and access to sufficient resources and services  
14 in diminishing neural vulnerability and promoting neural resilience to LLD,  
15 respectively. Our findings therefore provide insights into preventive strategies for  
16 LLD, and thus are of importance for policy makers as well as the broader society.  
17  
18  
19  
20

## 21 **Introduction (529)**

22 Late life depression (i.e., depression in older adults aged 60+; LLD) has been  
23 associated with increased risks of disability and mortality (Schulz *et al.*, 2000). It  
24 is intertwined with conditions and factors that are primarily ageing-related,  
25 yielding distinctive and complex etiological and clinical profiles in contrast to  
26 depression in younger age groups (Blazer, 2003; Alexopoulos, Schultz and  
27 Lebowitz, 2005). Previous work has shown that risk factors such as physical  
28 disability, medical illness, cognitive impairment, worse socioeconomic status,  
29 greater exposures to traumatic events, less social support, and living an  
30 unhealthy lifestyle contribute to higher chances of depression (Blazer, 2003;  
31 Chang-Quan *et al.*, 2010; Chang *et al.*, 2016). However, these studies did not  
32 investigate individual variation in LLD vulnerability and/or resilience and how  
33 such variation may be linked to various risk factors. Quantifying LLD resilience  
34 and vulnerability in patients is of great clinical relevance as it may ultimately  
35 inform future interventions. Here we employed a novel approach to evaluate  
36 neural resilience and vulnerability to LLD at the individual level and determined  
37 whether known risk factors of LLD explain individual differences in such neural  
38 resilience and vulnerability.

39 In previous studies, LLD has been associated with abnormalities in structural and  
40 functional properties (Manning and Steffens, 2018). It has also been associated  
41 with accelerated brain age, the magnitude of which further showed a correlation  
42 with declined cognitive performance (Christman *et al.*, 2020). These findings  
43 demonstrate the potential of proxy measures that capture the neural  
44 underpinnings of the disorder. Here, we build on this prior work to assess  
45 resilience and vulnerability to depressive symptom severity, using similar  
46 aggregate neural measures. Specifically, we sought to quantify such resilience  
47 and vulnerability from neuroanatomical patterns that are related to recent  
48 depressive symptoms and to examine whether LLD risk factors could explain  
49 individual differences in the quantified neural resilience and vulnerability.  
50 Specifically, here we focused on a vulnerable group of older adults who have  
51 experienced at least one depression episode before the assessment in this  
52 study. This provides an opportunity to enhance the variance in depression  
53 symptom severity by including individuals along the spectrum of potential LLD.

54 Inspired by brain-age models that predict the age of the brain based on  
55 neuroanatomical features in healthy individuals (Franke and Gaser, 2019), here  
56 we predicted the individual-level brain-based depression score (BDS) from  
57 multimodal neuroimaging features ( $n=4,632$ ; see more details in *Materials and*  
58 *Methods*). The difference between the predicted BDS and the original symptom  
59 score (delta BDS;  $\Delta BDS$ ) was calculated to index “neural resilience” or “neural  
60 vulnerability” to LLD and then linked to a set of LLD risk factors that covered a  
61 wide range of sociopsychological, medical and lifestyle variables (see variable  
62 full list in *Materials and Methods*). We specifically focused on individuals with  
63 highest neural resilience or vulnerability (i.e., top 10% negative and positive  
64  $\Delta BDS$  respectively) that represent older adults with the greatest clinical  
65 relevance. In practice, the focus on these highly resilient and vulnerable  
66 individuals also minimized the correlations between  $\Delta BDS$  and original symptom

67 score (i.e., similar to correlations between brain-age delta and chronological age  
68 in brain-age literature; (Franke and Gaser, 2019; Smith *et al.*, 2019). This  
69 enabled us to identify risk factors showing unique associations with neural  
70 resilience and/or vulnerability.

71

## 72 **Materials and Methods**

73

### 74 Participants

75

76 Participants from the UK Biobank (UKB) dataset aged 60 or above at the time of  
77 imaging acquisition with a history of probable major depression status (i.e., prior  
78 experiences in single or recurrent depression episodes; (Smith *et al.*, 2013))  
79 were included to ensure sufficient variance in depression symptomatology  
80 ( $M_{\text{age}}=66.35$ ; 60.3% female). Approximately 70% ( $N=1,405$ ) of the resulting  
81 sample ( $N=1,988$ ) had a status of recurrent major depression. Due to missing  
82 data in risk factor variables, a sub-sample of  $N=1,464$  participants were included  
83 in partial correlation and quantile regression analyses with similar demographic  
84 characteristics and prior depression histories as in the full sample ( $M_{\text{age}}=66.18$ ;  
85 59.4% female; 70% recurrent MDD). All participants in this study provided  
86 informed consent. UK Biobank has ethical approval from the North West Multi-  
87 Centre Research Ethics Committee (MREC). Data access was obtained under  
88 UK Biobank application ID 47267.

89

### 90 Data acquisition and measurement

91

#### 92 *Depressive symptoms*

93 A touchscreen questionnaire was implemented to collect information on  
94 sociodemographic characteristics and mental health. Recent depressive  
95 symptoms were measured using four items (RDS-4) that assess depressed  
96 mood, disinterest, restlessness, and tiredness in the past two weeks (Dutt *et al.*,  
97 2022). This continuous measure is highly comparable to several standardized  
98 self-report depression scales including PHQ-9, CES-D, and MASQ-30 (Dutt *et al.*,  
99 2022), and shows an area under the curve of 0.79 for its correlation with  
100 depression diagnosis (Khubchandani *et al.*, 2016). In response to each of these  
101 four questions, participants indicated their experiences from “not at all” (scoring  
102 1) to “nearly every day” (scoring 4) such that the total symptom score ranged  
103 from 4 to 16.

104

#### 105 *Imaging preprocessing and multimodal imaging features*

106 All brain imaging data from the UKB were acquired using standard Siemens  
107 Skyra 3T scanners with a standard Siemens 32-channel RF receive head coil.  
108 Detailed information for UKB imaging acquisition can be found in the UK Biobank  
109 Imaging Documentation, hosted on the Oxford FMRIB UK Biobank resource  
110 page (<https://www.fmrib.ox.ac.uk/ukbiobank/>). A fully automated processing and  
111 QC pipeline was developed for UKB brain imaging data, which included T1, T2,  
112 FLAIR, susceptibility-weighted MRI, resting-state MRI, task-evoked MRI and

113 diffusion MRI (Alfaro-Almagro *et al.*, 2018). Additionally, this pipeline also  
114 generated a set of imaging-derived phenotypes (IDPs) such as cortical and  
115 subcortical structure volumes, microstructural measures in major tracts, and  
116 functional connectivity metrics. In this study, a total of 4,632 IDPs was included  
117 as multimodal imaging features in the prediction models for estimating brain-  
118 depression score (see section 3.1). Approximately three quarters of these  
119 features were derived from the resting-state and task-evoked fMRI data, and the  
120 remaining from structural and diffusion MRI data:

- 121 - Resting-state fMRI features: Amplitude of ICA100 nodes and ICA25  
122 nodes; Edges of full correlation matrix from ICA100 and ICA25; Edges of  
123 partial correlation matrix from ICA100
- 124 - Task-evoked fMRI features: Median and 90th percentile BOLD signals for  
125 shapes and faces, as well as shape-face contrasts using a group mask  
126 and an amygdala mask respectively; Median and 90th percentile Z-  
127 statistics for shapes and faces, as well as shape-face contrasts using a  
128 group mask and an amygdala mask respectively
- 129 - Structural MRI features: Volumes of cortical and subcortical (including  
130 sub-segments) structures; Total volume of white matter hyperintensities
- 131 - Diffusion MRI features: Mean FA, MD, MO, L1-L3, ICVF, OD, ISOVF  
132 based on Standardized FA Skeleton; Weighted-mean FA, MD, MO, L1-L3,  
133 ICVF, OD, ISOVF in White-matter tracts

134

#### 135 *Late-life Depression Risk factors*

136 A list of risk factors for late-life depression (LLD) was curated based on the  
137 literature that covers information on demographics, lifestyle, medical conditions,  
138 adverse experiences, and psychosocial factors. Measures of these variables  
139 were collected from participants either via a touchscreen questionnaire or a  
140 verbal medical history interview on the same day of imaging acquisition.  
141 Specifically, several variables such as self-reported health, long-standing illness  
142 and Townsend deprivation index, which is a census-based index of material  
143 deprivation calculated by the combination of four indicators of deprivation: non-  
144 home ownership, non-car ownership, unemployment and overcrowding  
145 (Townsend, Phillimore and Beattie, 1988) were available directly from the UKB,  
146 whereas aggregate measures for healthy lifestyle, sleep quality, vascular risk  
147 factors, adverse or traumatic experiences, social isolation and loneliness were  
148 derived using multiple items as follows:

- 149 - A *healthy lifestyle score* was constructed based on smoking status,  
150 physical activity, diet, and alcohol consumption that are well documented  
151 as depression risk factors (Sarris *et al.*, 2020; van Lee *et al.*, 2020; Kang  
152 *et al.*, 2021). Based on national recommendations, participants were given  
153 1 for healthy, and 0 for unhealthy behaviors. Detailed coding information  
154 can be found in (Lourida *et al.*, 2019).
- 155 - A *sleep (low) risk score* was calculated using five sleep questions. Low-  
156 risk sleep factors were defined as a) having an early chronotype, b)  
157 sleeping 7–8 hours per day, c) never having or rarely having insomnia  
158 symptoms, d) not reporting snoring, and e) not reporting frequent daytime

159 sleepiness (Fan *et al.*, 2020). Participants received a score of 1 if their  
160 behaviors were classified as low risk for that factor and a sum score was  
161 calculated across five factors, where higher scores represent healthier  
162 sleep patterns or low risks of sleep issues (Hepsomali and Groeger,  
163 2021).

- 164 - An *aggregate measure of vascular risk factors* was calculated for each  
165 participant by counting instances of having a high BMI (>25), having a  
166 high waist-hip ratio (WHR>0.85 for females and WHR>0.90 for males),  
167 having ever smoked, and a self-reported diagnosis of hypertension,  
168 diabetes, or hypercholesterolemia (Cox *et al.*, 2019). The resulting sum  
169 score of instances represent potential vascular risks, where higher scores  
170 indicating higher risks.
- 171 - scores were calculated separately for childhood, adulthood, and lifetime  
172 experiences with dichotomization of responses to each individual question  
173 (Yapp *et al.*, 2021). Specifically, responses of “never true” to negative  
174 experiences (e.g., hit hard) scored a 0 and responses of “rarely true” and  
175 more often (i.e., “sometimes true”, “often”, “very often true”) scored a 1,  
176 which was reversed for positive experiences (e.g., in a confiding  
177 relationship). Binary responses (“yes”, “no”) were scored 1 and 0  
178 respectively. Separate sum scores were calculated to indicate the  
179 magnitude of traumatic experiences in different time periods and included  
180 as separate predictors in the models.
- 181 - *Psychosocial factors* comprised two measures: loneliness and social  
182 isolation. Participants were classified as lonely if they reported feeling  
183 lonely often and if they could confide to someone close only occasionally  
184 (e.g., less than once every few months), and socially isolated if they met at  
185 least two criteria of 1) living alone, 2) visiting their family or friends less  
186 than once a month, and 3) participating in none of the listed leisure/social  
187 activities (Mutz, Roscoe and Lewis, 2021). These psychosocial factors  
188 were included in statistical models as separate predictors.

## 189 190 191 Statistical analysis

### 192 193 *Estimating the delta of brain-depression score*

194 Our approach was inspired by the estimation of brain-age delta from  
195 neuroimaging features that is defined as the difference between the estimated  
196 brain age and chronological age in a given individual, which has been used to  
197 indicate underlying problems in outwardly healthy people and related to the risk  
198 of cognitive ageing or age-associated brain disease (Franke *et al.*, 2010; Cole  
199 and Franke, 2017; Baecker *et al.*, 2021). In this study, we employed Multivariate  
200 Adaptive Regression Splines models (Friedman and Roosen, 1995; Friedman,  
201 2007) to estimate the brain-depression score (BDS) as informed by multimodal  
202 imaging features and quantified the difference between the estimated and the  
203 actual depression symptom scores (i.e.,  $\Delta BDS$ ), with a positive  $\Delta BDS$  indicating  
204 neural vulnerability to depression (i.e., actual reported symptom score higher

205 than BDS) and negative  $\Delta BDS$  indicating neural resilience to depression (i.e.,  
206 actual symptom score lower than BDS).

207 Multivariate Adaptive Regression Splines (MARS) is a flexible regression  
208 technique that can capture the intrinsic nonlinear and multidimensional  
209 relationship of variables with an ensemble of linear functions joined together by  
210 one or more spline basis functions, where the number of basis functions and the  
211 parameters associated with each function (e.g., product degree and knot  
212 locations) are determined by the data (Friedman and Roosen, 1995; Friedman,  
213 2007). Specifically, MARS builds a model in two phases: the forward pass and  
214 the backward pruning, similar to growing and pruning of tree models. In the  
215 forward pass, MARS starts with a model consisting of just the intercept term (i.e.,  
216 the mean of the response values), followed by the assessment of every single  
217 predictor to find a basis function pair that produces the maximum improvement in  
218 the model error. This process iterates until either the model reaches a predefined  
219 limit number of terms, or the error improvement reaches a predefined limit. The  
220 result of the forward pass is a MARS basis matrix with rows of observations and  
221 columns of basis functions (e.g., hinge functions). To avoid overfitting by the full  
222 terms in the basis matrix from the forward pass, the backward pass is to find the  
223 subset of these terms that gives the best generalized cross validation (GCV) via  
224 a stepwise term deletion procedure. This backward pruning process continues  
225 until only one term remains (the intercept term) and the final model with the best  
226 GCV is selected (Friedman and Roosen, 1995; Friedman, 2007).

227 In this study, IDPs from multimodal imaging data and depressive symptom  
228 sum scores were included in MARS models as independent ( $X$ ) and dependent  
229 ( $Y$ ) variables. Additionally, age, sex, head size, head motion (i.e., the averaged  
230 head motion across space and time points) during fMRI acquisition (i.e., for both  
231 the resting-state and task-evoked fMRI), scanner site, scanner table position and  
232 data acquisition dates were included in all MARS models as confounding  
233 variables. Per partition of the full data in the nested cross-validations (see details  
234 below), principal component analysis (PCA) was employed to decompose high-  
235 dimensional  $X$  and components collectively explaining more than 50% variance  
236 were retained. As the outcome measure  $Y$  (i.e., symptom sum score) in our study  
237 is highly skewed with a long tail, transformation of  $Y$  was performed per data  
238 partition before modeling to enforce Gaussianity. This was realized by using a  
239 data-drive approach that finds the optimal normalization method from a suite of  
240 possible transformation options including the Box-Cox transformation, Yeo-  
241 Johnson transformation, the ordered quantile technique, Arcsinh transformation,  
242 exponential transformation, square root transformation and the Lambert  $W \times F$   
243 transformation (Peterson, 2021). We also applied dummy coding for all factorial  
244 variables such as sex and scanner site before data partitioning to ensure the  
245 same number of predictors across models.

246 Nested cross-validations were applied to increase robustness and  
247 generalizability of our MARS estimations, with 3 iterations in the outer loop and  
248 10 folds per iteration in the inner loop. As mentioned earlier, data processing  
249 including PCA (on  $X$ ) and transformation (on  $Y$ ) was performed within each  
250 iteration of the outer loop and parameters obtained from the training and

251 validating set were applied to the held-out testing set. Per training fold, a grid  
252 search was performed to identify the optimal combination of two parameters: the  
253 maximum degree of interactions among terms (*ndegree*) and the number of  
254 terms retained in the final model (*nprune*). Given the available data points and  
255 the empirical evidence that 3<sup>rd</sup>-degree interactions never benefited model fit  
256 using a subset of data, expansion of interaction degree was restricted to 2 (e.g.,  
257 testing *ndegree* = 1 and = 2) and *nprune* up to 5 times of the predictor numbers  
258 (i.e., varied between 690 and 695 due to changing numbers of principal  
259 components in each fold). Per prediction model on the testing set, we further  
260 partitioned data to estimate prediction uncertainty as the noise and model  
261 variance of the out-of-fold predicted values over 5 iterations of 50 cross-  
262 validations, using variance models of MARS (Milborrow, 2015), and an averaged  
263 r-squared of 0.19 in contrast to 0.09 from the training models.

264 For each participant, we quantified  $\Delta BDS$  as the difference between the  
265 predicted BDS ( $\hat{y}$ ) and the reported symptom sum score ( $Y$ ) while accounting for  
266 the prediction uncertainty including irreducible “aleatoric” or noise variance ( $\sigma_a^2$ )  
267 and model variance of prediction or “epistemic” uncertainty ( $\sigma_e^2$ ) such that  
268  $\Delta BDS = \frac{Y - \hat{y}}{\sqrt{\sigma_a^2 + \sigma_e^2}}$ . By definition, the resulting  $\Delta BDS$  for each participant indexed

269 less depressed or resilient brain patterns if the quantity was negative, and more  
270 depressed or vulnerable brain patterns if positive. Here, we focused on  
271 individuals with high neural resilience (i.e., top 10 percentile of the negative  
272  $\Delta BDS$ ) and individuals with high neural vulnerability (i.e., top 10 percentile of the  
273 positive  $\Delta BDS$ ). This was determined to drive a good balance between sufficient  
274 statistical power (i.e.,  $n = 144$  with 11 regressors) and high clinical relevance, and  
275 to reduce dependency of BDS as a function of original symptom score (i.e.,  
276 minimize high correlation between  $\Delta BDS$  and original symptom score).

277

### 278 *Testing risk factor effects*

279 All analyses were conducted for individuals with high neural resilience and  
280 vulnerability separately. We first conducted partial rank correlation analyses to  
281 test the associations between each risk factor and the  $\Delta BDS$  while controlling for  
282 the reported symptom sum score (i.e., resulting in effects not influenced by the  
283 sum score). This is a common practice to deconfound the associative effects  
284 driven by chronological age rather than the brain-age delta in the brain age  
285 literature (Smith *et al.*, 2019). False Discover Rate (FDR) corrections were  
286 applied to adjust for multiple testing. We further conducted quantile regression  
287 analyses to identify unique contributions of individual risk factors, while  
288 accounting for the effects of reported symptom sum score.

289

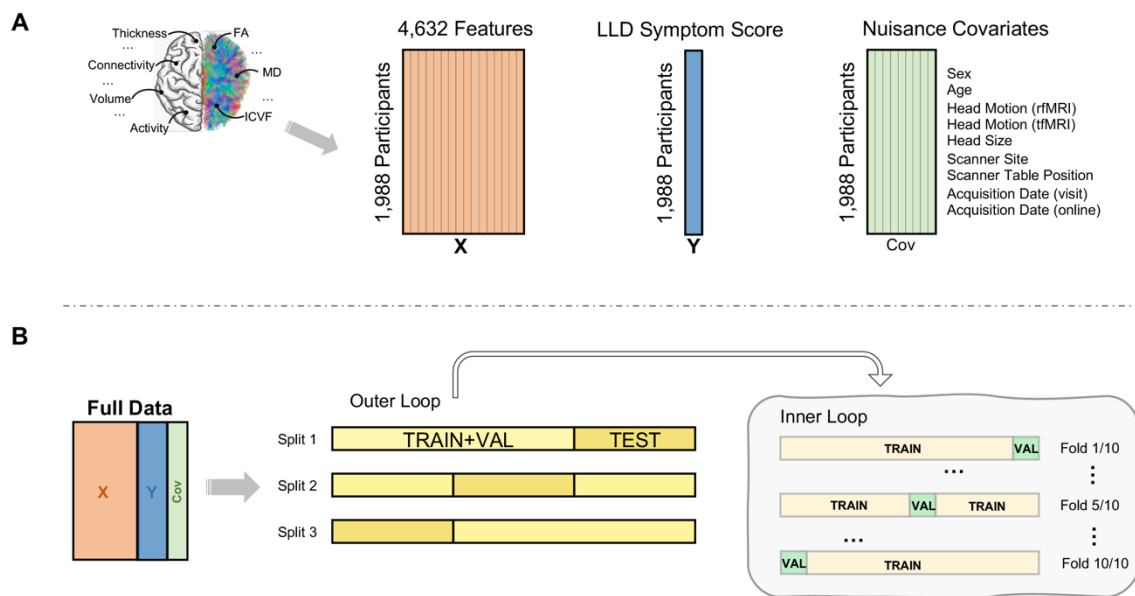
290

## 291 **Results (289)**

292 For each participant, we estimated the BDS using the Multivariate Adaptive  
293 Regression Splines (MARS) model (*Figure 1*). Our model yielded successful  
294 prediction of the BDS from the held-out sample via nested cross validations  
295 (RMSE=0.90,  $R^2=0.09$ ), with a comparable effect size to recent brain-wide



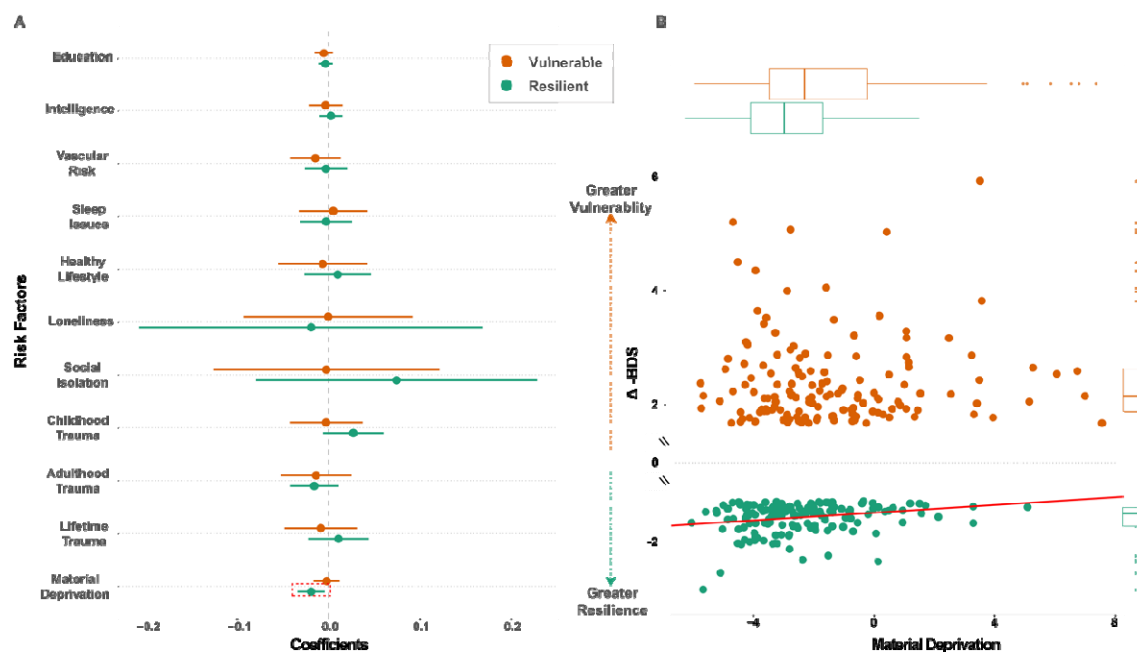
296 association studies that had sufficiently large sample sizes (Dick *et al.*, 2021;  
 297 Marek *et al.*, 2022). Importantly, our MARS model captures information about  
 298 brain structural and functional features associated with LLD symptoms and thus  
 299 indicates the disorder manifestation at the neurobiological level (i.e., a proxy of  
 300 how “depressed” an individual’s brain is).  
 301



302  
 303  
 304 **Figure 1. Prediction Models for Brain-depression Score.** (A) Multimodal imaging features  
 305 including cortical thickness, functional connectivity, gray matter volume, task activity and white  
 306 matter microstructure measures including fractional anisotropy (FA), mean diffusivity (MD) and  
 307 intracellular volume fraction (ICVF), as well as late-life depressive (LLD) symptom score and  
 308 nuisance covariates were included into multivariate adaptive regression splines models. (B) In  
 309 each model, multimodal imaging features (*X*) were used to predict symptom sum score (*Y*) while  
 310 controlling for sex, age, in-scanner motion, head size, scanner site, scanner table position and data  
 311 acquisition dates (*Cov*), via nested cross-validations. In the outer loop, full data were partitioned  
 312 into 3 splits and in the inner loop, each split of training and validating set (TRAIN+VAL) was fed  
 313 into a 10-fold cross-validation to validate the model.  
 314  
 315

316 In this study sample, about 58% ( $n=1,144$ ) participants appeared to possess a  
 317 resilient brain as their BDS was lower than their reported depressive symptom  
 318 scores (i.e., negative  $\Delta BDS$ ), and 42% showed the opposite pattern with a  
 319 vulnerable brain (i.e., positive  $\Delta BDS$ ). Results from partial correlation analyses  
 320 show that the Townsend deprivation index was negatively correlated with the  
 321 magnitude of neural resilience after FDR corrections ( $r=-0.26$ , FDR corrected  
 322  $p=0.018$ ). Findings from quantile regression analyses further show that this effect  
 323 is mostly robust in participants with the highest level of neural resilience (e.g., top  
 324 10 percentile with the largest negative  $\Delta BDS$ ) when all risk factors were  
 325 considered in one model ( $t=3.72$ ,  $p<0.001$ ; *Figure 2*). Interestingly, this  
 326 association with the material deprivation was not observed for individuals with the  
 327 highest neural vulnerability (i.e., top 10 percentile with the largest positive  $\Delta BDS$ ).

328 Neither did we observe this associative effect for the self-reported depressive  
329 symptom scores from individuals with the most resilient or vulnerable neural  
330 patterns. These findings together suggested a specific effect of material  
331 deprivation on the LLD-related neural resilience. Additionally, we observed a  
332 positive association between social isolation and the median quantile magnitude  
333 of neural vulnerability with adjustment for all other risk factors ( $t=2.01$ ,  $p<0.05$ ).  
334 This associative effect was absent in participants showing resilient patterns at the  
335 neuroanatomical level.  
336



337  
338 **Figure 2. Impact of Risk factors on Brain-depression Index.** (A) The dot-and-whisker plot  
339 compares the estimated coefficient and its standard error for each risk factor from separate  
340 multiple linear regression models for high neural resilience and vulnerability. (B) Material  
341 deprivation was significantly associated with the delta of brain-depression score ( $\Delta BDS$ ) only for  
342 individuals with high neural resilience.  
343  
344

### 345 Discussion (312)

346 In this study, we quantified individual-specific neural resilience and vulnerability  
347 to LLD using multimodal imaging features and linked known risk factors of LLD to  
348 such neural resilience and vulnerability. Our findings provide empirical evidence  
349 that risk factors may exert varying impact on the neurobiological manifestation of  
350 LLD. Specifically, we found a negative association between material deprivation and the  $\Delta BDS$   
351 in individuals with high neural resilience. This result indicated a beneficial effect of  
352 sufficient material resources on neural resilience to LLD. Interestingly, on the other hand,  
353 more material deprivation was not associated with neural vulnerability, suggesting that  
354 insufficient material resources alone may not adequately contribute to the differential  
355 patterns of brain structure and function that put individuals at increased risks of  
356 depression. Additionally, we observed a positive association between neural vulnerability  
357 to LLD and social

358 isolation, which was absent in participants showing neuroanatomically resilient  
359 patterns. These findings are consistent with the observations that older adults  
360 with sufficient resources to age successfully are relatively healthy, active,  
361 independent and maintain high levels of mental well-being (Terraneo, 2021), and  
362 that increases in socioeconomic status decreases the odds for depression  
363 (Freeman *et al.*, 2016; Zhou *et al.*, 2021). Furthermore, our results also resonate  
364 with previous findings that social isolation and/or loneliness in older adults is  
365 associated with increased risk of all-cause mortality (Holt-Lunstad *et al.*, 2015),  
366 as well as clinically significant depression and anxiety (Schwarzbach *et al.*, 2014;  
367 Taylor *et al.*, 2018; Domènech-Abella *et al.*, 2019; Donovan and Blazer, 2020).  
368 It is however, important to note that the BDS was estimated from the symptom  
369 sum score in the current study and thus might fail to capture subtleties in  
370 neuroanatomical features associated with specific clinical subtypes. It is highly  
371 likely that the disorder manifests in a heterogenous manner and the presentation  
372 of vulnerability at the neuroanatomical level can vary across individuals. Future  
373 studies may consider using individual symptom-level or dimensional measures of  
374 LLD to estimate BDS and test risk factor effects on those potential subtypes.  
375 In conclusion, our results demonstrate a link between material deprivation and  
376 neural resilience, as well as between social isolation and neural vulnerability to  
377 LLD. These results are of importance for policy makers as well as the broader  
378 society, as they provide evidence that sufficient material resources can improve  
379 neural resilience to depression for older adults and that compensational solutions  
380 to improve human interactions are in urgent need to offset the potential  
381 vulnerability to LLD when in-person social contacts are restricted.

382  
383

384

### 385 **Acknowledgments**

386

387 This research was performed under UK Biobank application number 47267. This  
388 research was supported by the NIH (1 R34 NS118618-01) and the McDonnell  
389 Center for Systems Neuroscience.

390

391

## 392 **References**

- 393 Alexopoulos, G. S., Schultz, S. K. and Lebowitz, B. D. (2005) 'Late-Life Depression: A  
394 Model for Medical Classification', *Biological Psychiatry*. Elsevier, 58(4), p. 283. doi:  
395 10.1016/J.BIOPSYCH.2005.04.055.
- 396 Alfaro-Almagro, F. *et al.* (2018) 'Image processing and Quality Control for the first  
397 10,000 brain imaging datasets from UK Biobank', *NeuroImage*. doi:  
398 10.1016/j.neuroimage.2017.10.034.
- 399 Baecker, L. *et al.* (2021) 'Machine learning for brain age prediction: Introduction to  
400 methods and clinical applications', *EBioMedicine*. doi: 10.1016/j.ebiom.2021.103600.
- 401 Blazer, D. G. (2003) 'Depression in Late Life: Review and Commentary', *The Journals of*  
402 *Gerontology: Series A*. Oxford Academic, 58(3), pp. M249–M265. doi:  
403 10.1093/GERONA/58.3.M249.
- 404 Chang-Quan, H. *et al.* (2010) 'Education and risk for late life depression: A meta-  
405 analysis of published literature', *International Journal of Psychiatry in Medicine*. doi:  
406 10.2190/PM.40.1.i.
- 407 Chang, S. C. *et al.* (2016) 'Risk factors for late-life depression: A prospective cohort  
408 study among older women', *Preventive Medicine*. doi: 10.1016/j.ypmed.2016.08.014.
- 409 Christman, S. *et al.* (2020) 'Accelerated brain aging predicts impaired cognitive  
410 performance and greater disability in geriatric but not midlife adult depression',  
411 *Translational Psychiatry*. doi: 10.1038/s41398-020-01004-z.
- 412 Cole, J. H. and Franke, K. (2017) 'Predicting Age Using Neuroimaging: Innovative Brain  
413 Ageing Biomarkers', *Trends in Neurosciences*. doi: 10.1016/j.tins.2017.10.001.
- 414 Cox, S. R. *et al.* (2019) 'Associations between vascular risk factors and brain MRI  
415 indices in UK Biobank', *European Heart Journal*. doi: 10.1093/eurheartj/ehz100.
- 416 Dick, A. S. *et al.* (2021) 'Meaningful associations in the adolescent brain cognitive  
417 development study', *NeuroImage*. doi: 10.1016/j.neuroimage.2021.118262.
- 418 Domènech-Abella, J. *et al.* (2019) 'Anxiety, depression, loneliness and social network in  
419 the elderly: Longitudinal associations from The Irish Longitudinal Study on Ageing  
420 (TILDA)', *Journal of Affective Disorders*. doi: 10.1016/j.jad.2018.12.043.
- 421 Donovan, N. J. and Blazer, D. (2020) 'Social Isolation and Loneliness in Older Adults:  
422 Review and Commentary of a National Academies Report', *American Journal of*  
423 *Geriatric Psychiatry*. doi: 10.1016/j.jagp.2020.08.005.
- 424 Dutt, R. K. *et al.* (2022) 'Mental health in the UK Biobank: A roadmap to self-report  
425 measures and neuroimaging correlates', *Human Brain Mapping*. doi:  
426 10.1002/hbm.25690.
- 427 Fan, M. *et al.* (2020) 'Sleep patterns, genetic susceptibility, and incident cardiovascular  
428 disease: A prospective study of 385 292 UK biobank participants', *European Heart*  
429 *Journal*. doi: 10.1093/eurheartj/ehz849.
- 430 Franke, K. *et al.* (2010) 'Estimating the age of healthy subjects from T1-weighted MRI  
431 scans using kernel methods: Exploring the influence of various parameters',  
432 *NeuroImage*. doi: 10.1016/j.neuroimage.2010.01.005.
- 433 Franke, K. and Gaser, C. (2019) 'Ten years of brainage as a neuroimaging biomarker of  
434 brain aging: What insights have we gained?', *Frontiers in Neurology*. doi:  
435 10.3389/fneur.2019.00789.
- 436 Freeman, A. *et al.* (2016) 'The role of socio-economic status in depression: Results from  
437 the COURAGE (aging survey in Europe)', *BMC Public Health*. doi: 10.1186/s12889-016-  
438 3638-0.
- 439 Friedman, J. H. (2007) 'Multivariate Adaptive Regression Splines', *The Annals of*  
440 *Statistics*. doi: 10.1214/aos/1176347963.
- 441 Friedman, J. H. and Roosen, C. B. (1995) 'An introduction to multivariate adaptive  
442 regression splines', *Statistical Methods in Medical Research*. doi:

- 443 10.1177/096228029500400303.
- 444 Hepsomali, P. and Groeger, J. A. (2021) 'Diet, sleep, and mental health: Insights from
- 445 the uk biobank study', *Nutrients*. doi: 10.3390/nu13082573.
- 446 Holt-Lunstad, J. *et al.* (2015) 'Loneliness and Social Isolation as Risk Factors for
- 447 Mortality: A Meta-Analytic Review', *Perspectives on Psychological Science*. doi:
- 448 10.1177/1745691614568352.
- 449 Kang, M. *et al.* (2021) 'The relationship of lifestyle risk factors and depression in Korean
- 450 adults: A moderating effect of overall nutritional adequacy', *Nutrients*. doi:
- 451 10.3390/nu13082626.
- 452 Khubchandani, J. *et al.* (2016) 'The Psychometric Properties of PHQ-4 Depression and
- 453 Anxiety Screening Scale Among College Students', *Archives of Psychiatric Nursing*. doi:
- 454 10.1016/j.apnu.2016.01.014.
- 455 van Lee, L. *et al.* (2020) 'Multiple modifiable lifestyle factors and the risk of perinatal
- 456 depression during pregnancy: Findings from the GUSTO cohort', *Comprehensive*
- 457 *Psychiatry*. doi: 10.1016/j.comppsy.2020.152210.
- 458 Lourida, I. *et al.* (2019) 'Association of Lifestyle and Genetic Risk With Incidence of
- 459 Dementia', *JAMA*, 322(5), p. 430. doi: 10.1001/jama.2019.9879.
- 460 Manning, K. J. and Steffens, D. C. (2018) 'State of the Science of Neural Systems in
- 461 Late-Life Depression: Impact on Clinical Presentation and Treatment Outcome', *Journal*
- 462 *of the American Geriatrics Society*. NIH Public Access, 66(Suppl 1), p. S17. doi:
- 463 10.1111/JGS.15353.
- 464 Marek, S. *et al.* (2022) 'Reproducible brain-wide association studies require thousands
- 465 of individuals', *Nature*. Springer US, 603(7902), pp. 654–660. doi: 10.1038/s41586-022-
- 466 04492-9.
- 467 Milborrow, S. (2015) 'Notes on the earth package [WWW Document]', URL <http://www.milbo.org/doc/earth-notes.pdf>, pp. 1–69.
- 468 Mutz, J., Roscoe, C. J. and Lewis, C. M. (2021) 'Exploring health in the UK Biobank:
- 470 associations with sociodemographic characteristics, psychosocial factors, lifestyle and
- 471 environmental exposures', *BMC Medicine*. doi: 10.1186/s12916-021-02097-z.
- 472 Peterson, R. A. (2021) 'Finding Optimal Normalizing Transformations via bestNormalize',
- 473 *R Journal*. doi: 10.32614/rj-2021-041.
- 474 Sarris, J. *et al.* (2020) 'Multiple lifestyle factors and depressed mood: a cross-sectional
- 475 and longitudinal analysis of the UK Biobank (N = 84,860)', *BMC Medicine*. doi:
- 476 10.1186/s12916-020-01813-5.
- 477 Schulz, R. *et al.* (2000) 'Association between depression and mortality in older adults:
- 478 The Cardiovascular Health study', *Archives of Internal Medicine*. doi:
- 479 10.1001/archinte.160.12.1761.
- 480 Schwarzbach, M. *et al.* (2014) 'Social relations and depression in late life - A systematic
- 481 review', *International Journal of Geriatric Psychiatry*. doi: 10.1002/gps.3971.
- 482 Smith, D. J. *et al.* (2013) 'Prevalence and characteristics of probable major depression
- 483 and bipolar disorder within UK Biobank: Cross-sectional study of 172,751 participants',
- 484 *PLoS ONE*, 8(11), pp. 1–7. doi: 10.1371/journal.pone.0075362.
- 485 Smith, S. M. *et al.* (2019) 'Estimation of brain age delta from brain imaging',
- 486 *NeuroImage*. doi: 10.1016/j.neuroimage.2019.06.017.
- 487 Taylor, H. O. *et al.* (2018) 'Social Isolation, Depression, and Psychological Distress
- 488 Among Older Adults', *Journal of Aging and Health*. doi: 10.1177/0898264316673511.
- 489 Terraneo, M. (2021) 'The Effect of Material and Social Deprivation on Well-Being of
- 490 Elderly in Europe', *International Journal of Health Services*. doi:
- 491 10.1177/0020731420981856.
- 492 Townsend, P., Phillimore, P. and Beattie, A. (1988) *Health and deprivation: Inequality*
- 493 *and the North*. Edited by P. Townsend, P. Phillimore, and A. Beattie. London: Croom

494 Helm.  
495 Yapp, E. *et al.* (2021) 'Sex differences in experiences of multiple traumas and mental  
496 health problems in the UK Biobank cohort', *Social Psychiatry and Psychiatric  
497 Epidemiology*. doi: 10.1007/s00127-021-02092-y.  
498 Zhou, S. *et al.* (2021) 'Socioeconomic status and depressive symptoms in older people  
499 with the mediation role of social support: A population-based longitudinal study',  
500 *International Journal of Methods in Psychiatric Research*. doi: 10.1002/mpr.1894.  
501  
502  
503